IVYSPRING INTERNATIONAL PUBLISHER

Theranostics

2017; 7(8): 2277-2286. doi: 10.7150/thno.19257

Research Paper

Boosting the Peroxidase-Like Activity of Nanostructured Nickel by Inducing Its 3+ Oxidation State in $LaNiO_3$ Perovskite and Its Application for Biomedical Assays

Xiaoyu Wang[1], Wen Cao[1], Li Qin[1], Tingsheng Lin[2], Wei Chen[2], Shichao Lin[1], Jia Yao[1], Xiaozhi Zhao[2], Min Zhou[1], Cheng Hang[3], and Hui Wei[1, 4]✉

1. Department of Biomedical Engineering, College of Engineering and Applied Sciences, Collaborative Innovation Center of Chemistry for Life Sciences, Nanjing National Laboratory of Microstructures, Nanjing University, Nanjing, Jiangsu, 210093, China;
2. Department of Urology, Nanjing Drum Tower Hospital, the Affiliated Hospital of Nanjing University Medical School, Nanjing, Jiangsu, 210008, China;
3. State Key Laboratory of Coordination Chemistry, School of Chemistry and Chemical Engineering, Nanjing University, Nanjing 210093, China;
4. State Key Laboratory of Analytical Chemistry for Life Science, School of Chemistry and Chemical Engineering, Nanjing University, Nanjing 210093, China.

✉ Corresponding author: weihui@nju.edu.cn; Fax: +86-25-83594648; Tel: +86-25-83593272; Web: http://weilab.nju.edu.cn.

Received: 2017.01.19; Accepted: 2017.03.22; Published: 2017.06.01

Abstract

Catalytic nanomaterials with intrinsic enzyme-like activities, called nanozymes, have recently attracted significant research interest due to their unique advantages relative to natural enzymes and conventional artificial enzymes. Among the nanozymes developed, particular interests have been devoted to nanozymes with peroxidase mimicking activities because of their promising applications in biosensing, bioimaging, biomedicine, etc. Till now, lots of functional nanomaterials have been used to mimic peroxidase. However, few studies have focused on the Ni-based nanomaterials for peroxidase mimics. In this work, we obtained the porous $LaNiO_3$ nanocubes with high peroxidase-like activity by inducing its 3+ oxidation state in $LaNiO_3$ perovskite and optimizing the morphology of $LaNiO_3$ perovskite. The peroxidase mimicking activity of the porous $LaNiO_3$ nanocubes with Ni^{3+} was about 58~fold and 22~fold higher than that of NiO with Ni^{2+} and Ni nanoparticles with Ni^0. More, the porous $LaNiO_3$ nanocubes exhibited about 2-fold higher activity when compared with $LaNiO_3$ nanoparticles. Based on the superior peroxidase-like activity of porous $LaNiO_3$ nanocubes, facile colorimetric assays for H_2O_2, glucose, and sarcosine detection were developed. Our present work not only demonstrates a useful strategy for modulating nanozymes' activities but also provides promising bioassays for clinical diagnostics.

Key words: nanozymes, peroxidase-like activity, $LaNiO_3$ perovskite oxide, oxidation state, biomedical assays.

Introduction

Natural enzymes, with remarkable catalytic efficiency and extraordinary substrate specificity, have attracted researchers' enormous interest due to their important roles not only in living systems but also in biomedical diagnostics and therapeutics.[1] However, the intrinsic shortcomings of natural enzymes such as high cost, low stability, and difficulty of recycling have impeded their practical applications. To address these drawbacks, great efforts have been devoted to searching for natural enzymes' alternatives called as "artificial enzymes".[2-5] Recently, nanomaterials with enzyme-like characteristics, called as "nanozymes", have been developed to act as promising artificial enzymes along with the remarkable achievements in the field of nanotechnology.[6-9] As a new type of artificial enzymes, nanozymes are advantageous over natural enzymes in several aspects such as low cost,

long-term storage, and high stability. More, nanozymes are even superior to conventional artificial enzymes in their large surface area for bioconjugation, self-assembly capabilities, tunable catalytic activities, etc.[10-12] Therefore, intensive efforts have been devoted to developing functional nanomaterials for enzyme mimics in recent years.[13-27]

Among the nanozymes developed, particular interests have been focused on nanozymes with peroxidase mimicking activities due to their great promise in biomedical diagnosis, bioimaging, antibacterial agents, antibiofouling medical devices, etc.[28-38] Till now, lots of functional nanomaterials (e.g., carbon based, metal oxide based and metal based nanomaterials) have been explored to mimic peroxidase.[15, 17, 39-41] Among them, transition metal oxide nanomaterials had been extensively studied due to their excellent catalytic activities, high stability, low cost and ease of preparation.[6, 10, 11] For instance, Fe_3O_4 nanoparticles have been fabricated to mimic peroxidase for Ebola diagnosis and tumor immunostaining.[30, 42] Despite of these progresses, very little attention has been paid to developing Ni-based nanomaterials as peroxidase mimics. A recent study reported that NiO nanoparticles modified with H_2TCPP had an intrinsic peroxidase mimicking activity. However, the catalytic activity may be mainly from the H_2TCPP ligand rather than the NiO nanoparticle itself.[43] More, several seminal studies have demonstrated that the activities of nanozymes were strongly dependent on the size, composition, shape, surface ligand, and exposed facet of nanomaterials.[12, 44-49] Previous studies have also showed that the oxidation state was very important for cerium oxides' and iron oxides' enzyme mimicking activities.[50-53] However, very little information was available about the influence of nanostructured nickels' oxidation state on their enzyme mimicking activities. Such information, if available, would help to rationally design nanozymes with high enzyme mimicking activities (including peroxidase mimicking activities).

Here, we showed that high peroxidase mimicking activity of $LaNiO_3$ perovskite could be achieved by inducing the 3+ oxidation state of nickel into the perovskite lattice. To find out the effect of nickel atom's oxidation state on the Ni-based nanomaterials' peroxidase mimicking activity, other Ni-based nanomaterials such as NiO and Ni nanoparticles with Ni^{2+} and Ni^0 were also studied respectively. The peroxidase mimicking activity study revealed that the oxidation state of nickel in Ni-based nanomaterials was very important for the peroxidase mimicking activity and Ni^{3+} was superior to Ni^0 and Ni^{2+} for the nanozymes' catalytic activities. Specifically, the peroxidase mimicking activity of the porous $LaNiO_3$ was about 58~fold and 22~fold higher than that of NiO and Ni nanoparticles. More, the influence of $LaNiO_3$ morphology on its peroxidase-like activity was also investigated. The result showed that the peroxidase-like activities of porous $LaNiO_3$ nanocubes were about 2~fold higher than that of $LaNiO_3$ nanoparticles. The latter were synthesized by a conventional sol-gel method. Finally, the porous $LaNiO_3$ nanocubes with the highest peroxidase mimicking activity were employed to develop reliable diagnostic platforms for important biomolecular targets.

It has been established that bioactive small biomolecules, such as glucose and sarcosine, play critical roles in disease diagnosis.[54-58] For example, glucose is not only a well-known indicator for diabetes but also closely associated with ischemia stroke and even cancers.[59-65] Previous study also suggested that sarcosine may act as a metabolic biomarker for prostate cancer.[66] The oxidation of glucose and sarcosine with the corresponding oxidase produces H_2O_2. The produced H_2O_2 can catalytically oxidize peroxidase substrates with $LaNiO_3$ nanocubes-based peroxidase mimics to produce colored products for signaling. Therefore, we further developed facile bioassays for glucose and sarcosine detection by combining glucose oxidase (GOx) and sarcosine oxidase (SOx) with the porous $LaNiO_3$ nanocubes-based peroxidase mimics.

Materials and Methods

Chemicals and Materials

Nickel nitrate hexahydrate, citric acid, sucrose, and glucose were obtained from Nanjing Chemical Reagent Co., Ltd. Ethylene glycol, lactose, sodium hydroxide, hydrogen peroxide, and ammonium hydroxide were purchased from Sinopharm Chemical Reagent Co., Ltd. TMB (3,3′,5,5′-tetramethyl-benzidine), OPD (o-phenylenediamine), ABTS (2,2'-azino-bis(3-ethylbenzothiazoline-6-sulphonic acid)), fructose, glycine, lanthanum nitrate hexahydrate, lanthanum oxide, Ni nanoparticles, and glucose oxidase (GOx from Aspergillus niger, >180 units/mg) were purchased from Aladdin Chemical Reagent Co., Ltd. Polyvinyl pyrrolidone (PVP, molecular weight=58000) and sarcosine oxidase (SOx) were obtained from Sigma-Aldrich. All chemical reagents were used as received without further purification. Deionized water produced by Millipore system was used in all experiments.

Instrumentation

Powder X-ray diffraction (XRD) data were collected at room temperature on a Rigaku Ultima

diffractometer by using Cu Kα radiation. The diffractometer was operated at 40 kV and 40 mA with a scan rate of 2°/minute. Transmission electron microscopy (TEM) imaging was performed on a JEOL JEM-2100 transmission electron microscope at an acceleration voltage of 200 kV. Scanning electron microscopy (SEM) imaging was performed on a Hitachi S-4800 scanning electron microscope operating at 5 kV. UV-visible absorption spectra were collected on a UV-visible spectrophotometer (TU-9100, Beijing Purkinje General Instrument Co. Ltd., China). Nitrogen adsorption-desorption isotherms were performed on Micromeritics ASAP 2020 surface area and porosity analyzer, from which the nanozymes' surface areas were calculated with the Brunauer-Emmett-Teller (BET) method.

Synthesis of Porous $LaNiO_3$ Nanocubes via a Hydrothermal Method

$LaNiO_3$ nanocubes were synthesized as follows.[67] Briefly, the lanthanum nitrate hexahydrate (1.0 mmol), nickel nitrate hexahydrate (1.0 mmol), and glycine (4 mmol) were dissolved in 25 mL of deionized water, followed by the adding 0.3 g of PVP. After stirring for 30 min, the pH of the solution was adjusted to about 7.0 via slowly adding ammonium hydroxide. The resulting solution was transferred into a 40 mL Teflon-lined autoclave and heated at 180 °C for 24 hours. The resulting product was centrifuged and washed with deionized water and ethanol for several times, which was then dried at 60 °C for overnight. The precursor powder was finally annealed at 650 °C for 2 hours with a ramp rate of 5 °C/minute to obtain the final porous $LaNiO_3$ nanocubes.

Synthesis of $LaNiO_3$-H_2 Nanocubes

The $LaNiO_3$-H_2 was obtained by controlled reduction of as-prepared $LaNiO_3$ porous nanocubes with H_2 to partially form Ni^{2+} in the $LaNiO_3$-H_2 lattice. Specifically, the as-prepared $LaNiO_3$ was heated to 350 °C at a ramp rate of 5 °C/minute and maintained at 350 °C for 2 hours under a forming gas of 5% H_2 in Argon.

Synthesis of $LaNiO_3$-H_2-Air Nanocubes

To obtain the $LaNiO_3$-H_2-Air nanocubes, the as-prepared $LaNiO_3$-H_2 nanocubes were recalcined at 650 °C in the air for 2 hours with a ramp rate of 5 °C/minute.

Synthesis of $LaNiO_3$ Nanoparticles via a Sol-Gel Method

The $LaNiO_3$ nanoparticles were synthesized via a conventional sol-gel strategy.[68] Briefly, lanthanum nitrate hexahydrate (1.5 mmol), nickel nitrate hexahydrate (1.5 mmol), and citric acid (12 mmol) were dissolved in 100 mL of deionized water, followed by adding 1.5 mL of ethylene glycol. Subsequently, the resulting transparent solutions were condensed at 90 °C into a gel under stirring, which were then decomposed at 180 °C for 5 hours to form solid precursors. The solid precursors were then decomposed at 400 °C for 2 hours to obtain foam-like precursors via removing the organic components. The precursors were further annealed at 700 °C for 5 hours with a ramp rate of 5 °C/minute to obtain the final $LaNiO_3$ nanoparticles. The obtained $LaNiO_3$ nanoparticles was denoted as $LaNiO_3$-SG.

Synthesis of NiO

NiO nanoparticles were synthesized as follows.[69] 0.5 g of NaOH and 1.66 g of PVP were dissolved in 25 mL of deionized water and 1.45 g of nickel nitrate hexahydrate was dissolved in 10 mL of deionized water, respectively. The nickel nitrate aqueous solution was then added to the NaOH/PVP solution dropwise under stirring. The resulting solution was stirred for 3 hours to obtain the NiO precursor, followed by washing with H_2O and ethanol for several times and drying at 60 °C overnight. Then, the precursor was annealed at 650 °C for 2 hours in air with a ramp rate of 5 °C/minute to form the final NiO nanoparticles.

Colorimetric Detection of H_2O_2, Glucose, and Sarcosine with the Porous $LaNiO_3$ Nanocubes

H_2O_2 detection was carried out as follows: (1) 20 μL of porous $LaNiO_3$ nanocubes (1 mg/mL), 80 μL of TMB (10 mM), and 800 μL of NaOAc buffer (0.2 M, pH 4.5) was added into a 1.5 mL tube. (2) 100 μL of H_2O_2 with various concentrations was added into the above reaction solution. (3) The mixed solution was incubated for 20 min at 37 °C and then the absorption spectra were measured when keeping the solution in an ice water bath.

Glucose detection was performed as follows: (1) 100 μL of GOx (1 mg/mL) and 100 μL of glucose with different concentrations in 0.2 M phosphate buffer (pH 7.0) were incubated for 30 min at 37 °C. (2) 20 μL of porous $LaNiO_3$ nanocubes (1 mg/mL), 100 μL of TMB (10 mM), and 680 μL of NaOAc buffer (0.2 M, pH 4.5) were added into the above 200 μL of glucose and GOx reaction solution. (3) The mixed solution was incubated for 20 min at 37 °C and then the absorption spectra were measured when keeping the solution in an ice water bath.

Sarcosine detection was performed as follows: (1) 100 μL of SOx (2 mg/mL) and 100 μL of sarcosine with various concentrations in 0.2 M phosphate buffer (pH 7.0) were incubated for 90 min at 37 °C. (2) 60 μL

of porous $LaNiO_3$ nanocubes (1 mg/mL), 100 μL of TMB (10 mM), and 640 μL of NaOAc buffer (0.2 M, pH 4.5) was added into the above 200 μL sarcosine and SOx reaction solution. (3) The mixed solution was incubated for 20 min at 45 °C and then the absorption spectra were measured when keeping the solution in an ice water bath.

Cell Assays

Hela cells were incubated in High Glucose DMEM medium with 10% fetal bovine serum (FBS) at 37 °C with the atmosphere containing 5% CO_2. Fresh cells were subcultured into 96 wells, and 10 μg/mL lipopolysaccharides (LPS) was used to incubate with cells overnight. Then, 40 μg/mL $LaNiO_3$ and 0.5 mM TMB were added into the cells. The cells solution was incubated for 10 min and the absorbance values at 652 nm were measured.

Results and Discussion

Synthesis and Characterization of Porous $LaNiO_3$ Nanocubes

The porous $LaNiO_3$ nanocubes were obtained by annealing the nanocube-like precursors at 650 °C for 2 hours with a ramp rate of 5 °C/minute. The SEM images of nanocube-like precursors shown in Figure 1A and Figure S1A revealed that the precursors had smooth surfaces with the size of about 800 nm. After annealing in air at 650 °C for 2 hours, the annealed products maintained the precursors' nanocube-like morphology. The annealed products had rough surfaces with the size about 600 nm as shown in Figure 1B and Figure S1B. As shown in the SEM and TEM images of Figure 1B and Figure 1C, lots of pores randomly distributed in the annealed products after annealing the precursors in air at 650 °C for 2 hours. The high-resolution TEM images of the porous $LaNiO_3$ nanocubes showed in Figure S1D suggested that the annealed products were polycrystalline. As shown in Figure 1D, the distance of the adjacent fringes was 0.271 nm, which was corresponded to the lattice spacing of the (110) plane of $LaNiO_3$ perovskite. X-ray diffraction patterns confirmed that the annealed products had a perovskite structure with high phase purity, as seen in Figure 1E. This result suggested that nanocube-like precursors were completely transformed into porous $LaNiO_3$ perovskite oxide after annealing in air at 650 °C for 2 hours.

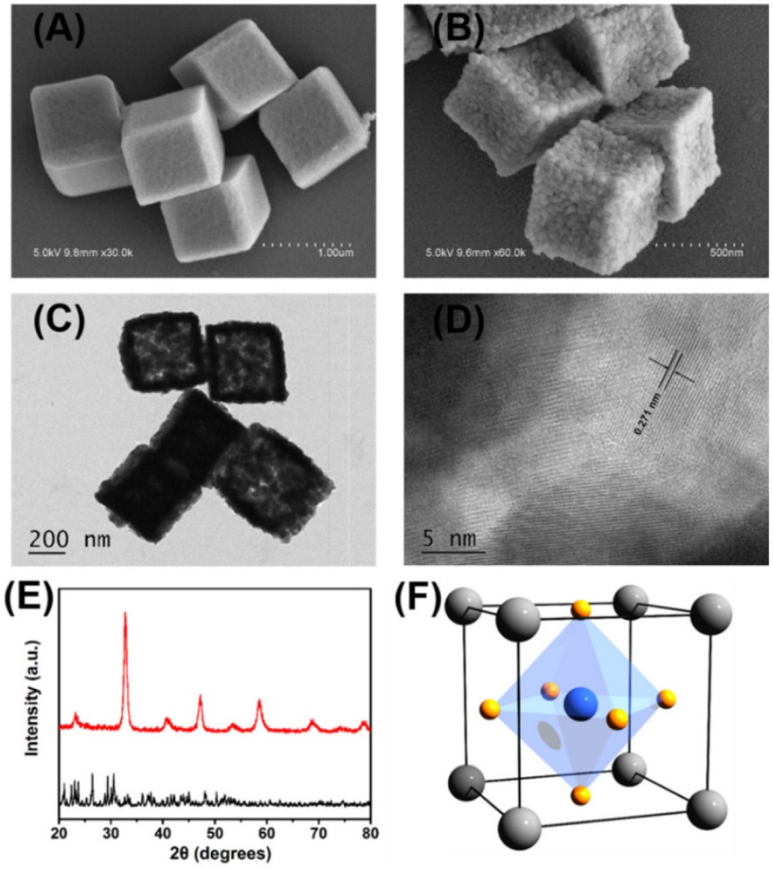

Figure 1. Representative SEM images of (A) the obtained nanocube-like precursors and (B) the porous $LaNiO_3$ nanocubes after annealing the precursors. (C) Representative TEM images of the porous $LaNiO_3$ nanocubes. (D) High-resolution TEM images of the porous $LaNiO_3$ nanocubes. (E) Powder X-ray diffraction patterns of the nanocube-like precursors (black line) and the porous $LaNiO_3$ nanocubes (red line). (F) Schematic of $LaNiO_3$ perovskite oxide structure (La in grey, Ni in blue, and O in yellow).

Evaluation of Peroxidase Mimicking Activity of Porous $LaNiO_3$ Nanocubes

After establishing the successful fabrication of the porous $LaNiO_3$ nanocubes, the peroxidase-like activity of the nanocubes was investigated. To evaluate the peroxidase mimicking activity of the porous $LaNiO_3$ nanocubes, TMB was selected as the catalytic substrate because it was a typical chromogenic substrate for peroxidase. The oxidation of TMB generated the oxidized product (i.e., TMBox) with characteristic absorption peaks at 370 nm and 652 nm. As seen in Figure 2, the porous $LaNiO_3$ nanocubes along with H_2O_2 and TMB incubated at room temperature for 10 min showed a deep blue color with strong absorbance at 370 nm and 652 nm. However, the other control experiments suggested that the solution contained TMB alone or H_2O_2 and TMB showed negligible color change. Note, the $LaNiO_3$ and TMB system also showed a slight color change, which was probably due to the oxidase mimicking activity of $LaNiO_3$ nanocubes. To further confirm the peroxidase-like activity of porous $LaNiO_3$ nanocubes, the colorimetric experiments were also performed with the other two typical peroxidase substrates (i.e., OPD and ABTS). As confirmed in Figure S2, all three peroxidase substrates showed deep color changes with strong absorbance, which were attributed to the catalytic oxidation of the substrates with the porous $LaNiO_3$ nanocubes in the presence of H_2O_2. These results confirmed that the porous $LaNiO_3$ nanocubes possessed peroxidase-like activity.

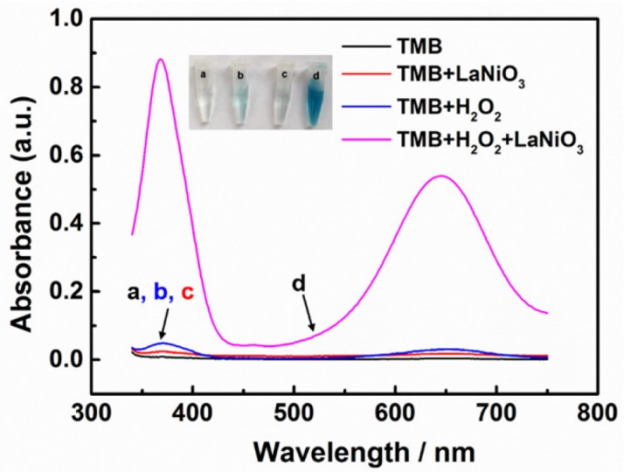

Figure 2. The absorption spectra of different reaction systems: (a) TMB only, (b) TMB + H_2O_2, (c) TMB + $LaNiO_3$ nanocubes, and (d) TMB + H_2O_2 + $LaNiO_3$ nanocubes.

The activity of nature enzymes is dependent on substrate concentrations and reaction conditions. Similar with the nature enzymes, the influence of H_2O_2 concentrations, catalyst concentrations, temperature, and pH on the peroxidase-like activity of the porous $LaNiO_3$ nanocubes was investigated. As seen in Figure 3A, the reaction rate increased with the increase of H_2O_2 concentrations, indicating that the peroxidase-like activity of porous $LaNiO_3$ nanocubes was dependent on the H_2O_2 concentrations. The effect of catalyst concentrations was also evaluated by monitoring the time-dependent absorption spectra under various catalyst concentrations. The reaction rate dramatically increased with the increase of catalyst concentrations, demonstrating that the peroxidase-like activity of porous $LaNiO_3$ nanocubes was dependent on the catalyst concentrations. More, the pH and temperature-dependent peroxidase-like activity were also investigated. As shown in Figure 3C, the peroxidase-like activity of porous $LaNiO_3$ nanocubes was gradually increased in the pH range from 1 to 4.5, while the peroxidase-like activity was gradually decreased in the pH range from 4.5 to 10. The effect of temperature on the peroxidase-like activity of $LaNiO_3$ nanocubes was evaluated in the range from 20 °C to 60 °C. The peroxidase-like activity was confirmed to be the optimal at 55 °C. In a word, the peroxidase-like activity of porous $LaNiO_3$ nanocubes was dependent on the pH and temperature and the optimized pH and temperature were 4.5 and 55 °C, respectively.

To investigate the catalytic mechanism and quantify the peroxidase-like activity of porous $LaNiO_3$ nanocubes, the apparent steady-state kinetic parameters for the oxidation of TMB and H_2O_2 were determined. The kinetic data were obtained by varying the concentration of one substrate of H_2O_2 or TMB while keeping the other's concentration constant. In the suitable concentration range of H_2O_2 and TMB, typical Michaelis-Menten curves were obtained (Figure 4). The important enzyme kinetic parameters of maximum initial velocity (V_{max}) and Michaelis-Menten constant (K_m) were obtained using the Lineweaver-Burk plot. K_m value showed the affinity of an enzymatic catalyst to its substrate, where the lower K_m value represented the higher affinity. V_{max} and K_m values of porous $LaNiO_3$ nanocubes, HRP, Pd-Ir cubes, graphene oxide (GO-COOH) and Fe_3O_4 were listed in Table S1. As seen in Table S1, the K_m value of porous $LaNiO_3$ nanocubes with H_2O_2 as the substrate was higher when compared to HRP, suggesting that the porous $LaNiO_3$ nanocubes had a lower affinity with H_2O_2 than HRP. Low affinity between nanozymes and H_2O_2 is common for the nanozymes with peroxidase-like activities (such as the metal-, metal oxide-, and carbon-based nanozymes in Table S1). Interestingly, the K_m value of porous $LaNiO_3$ nanocubes with TMB as the substrate was

lower when compared to HRP, which indicated the higher affinity between the porous $LaNiO_3$ nanocubes and TMB than HRP. It is noteworthy that the porous $LaNiO_3$ nanocubes showed higher V_{max} values for both H_2O_2 and TMB when compared to other peroxidase-like nanozymes previously reported (Table S1). This demonstrated the excellent peroxidase mimicking activities of the currently developed $LaNiO_3$ nanocubes.

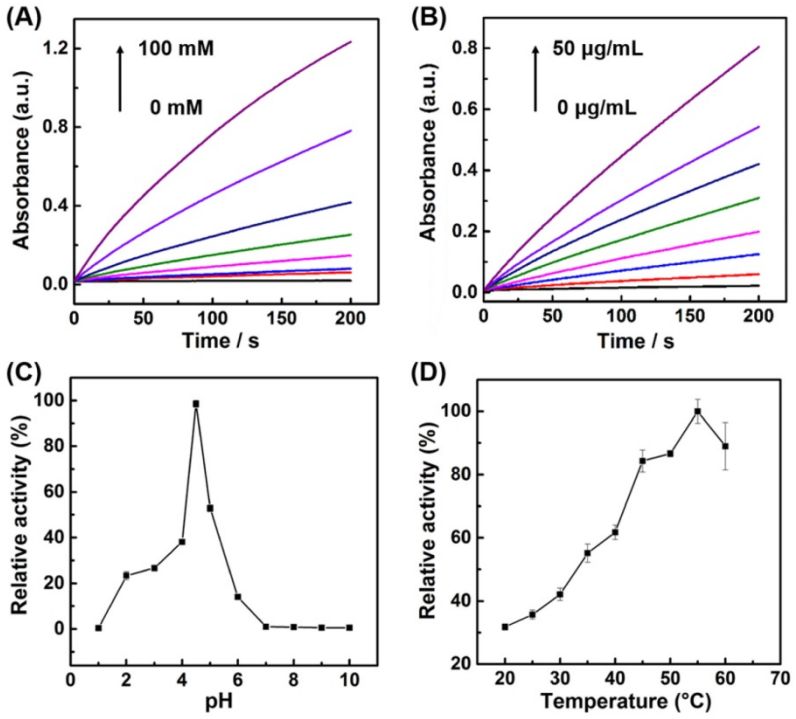

Figure 3. (A) Kinetic curves of A_{652} for monitoring the catalytic oxidation of 1 mM TMB with various concentrations of H_2O_2 in the presence of 10 μg/mL porous $LaNiO_3$ nanocubes. (B) Kinetic curves of A_{652} for monitoring the catalytic oxidation of 1 mM TMB with various concentrations of porous $LaNiO_3$ nanocubes in the presence of 10 mM H_2O_2. (C, D) pH and temperature-dependent peroxidase-like activities of the porous $LaNiO_3$ nanocubes.

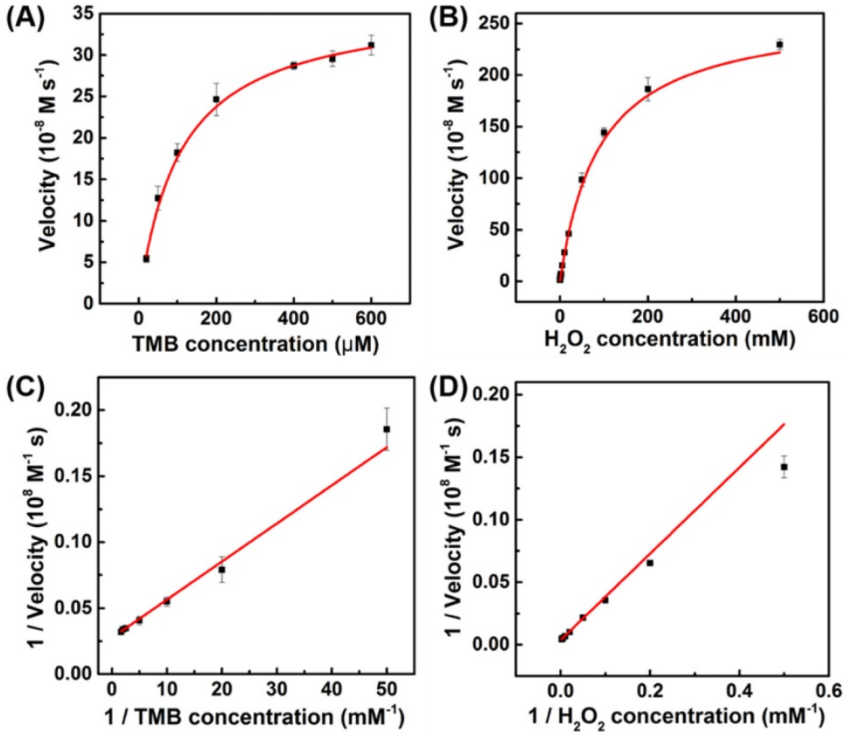

Figure 4. The steady-state kinetic assays of the porous $LaNiO_3$ nanocubes. Plots of the velocity of the reaction versus different concentrations of TMB (A, 10 mM H_2O_2) or H_2O_2 (B, 0.8 mM TMB). Double reciprocal plots of the velocity versus varying concentration of (C) TMB and (D) H_2O_2.

Comparison of the Peroxidase-Like Activity of Porous $LaNiO_3$ Nanocubes and Other Ni-based Nanomaterials

We investigated the influence of oxidation state of nickel atom in the Ni-based nanomaterials on their peroxidase-like activities. The peroxidase-like activities of Ni nanoparticles, $LaNiO_3$-H_2 nanocubes, and NiO with different oxidation state of nickel atom were studied and compared with that of the porous $LaNiO_3$ nanocubes. $LaNiO_3$-H_2 nanocubes were obtained by annealing the porous $LaNiO_3$ nanocubes at 350 °C for 2 hours under a forming gas with 5% H_2 in argon, which partially reduced the Ni^{3+} to Ni^{2+}. The successful synthesis of these Ni-based nanomaterials was confirmed by SEM and XRD (Figures S3-S6). The nickel atom in Ni nanoparticles was in the oxidation state of Ni^0, while the nickel atom in $LaNiO_3$ was Ni^{3+} and the nickel atom in NiO was Ni^{2+}. As shown in Figure 5A and Figure 5C, the porous $LaNiO_3$ nanocubes with Ni^{3+} exhibited the highest peroxidase-like activity while the Ni nanoparticles with Ni^0 and NiO with Ni^{2+} showed negligible peroxidase-like activities. Interestingly, the $LaNiO_3$-H_2 nanocubes exhibited about 71% peroxidase-like activity of $LaNiO_3$ nanocubes. The peroxidase-like activity of $LaNiO_3$-H_2 nanocubes decreased when compared to $LaNiO_3$ nanocubes because the Ni^{3+} was partially reduced to Ni^{2+} in $LaNiO_3$-H_2 nanocubes. These results demonstrated that the oxidation state of nickel atom was very important for the peroxidase-like activity of Ni-based nanomaterials. More, the Ni^{3+} can be an optimal oxidation state for Ni-based nanomaterials with peroxidase mimicking activity. It is noteworthy that the peroxidase-like activity of $LaNiO_3$-H_2 nanocubes can be recovered when the $LaNiO_3$-H_2 nanocubes were reoxidized at 650 °C for 2 hours under the air to form $LaNiO_3$-H_2-Air. The peroxidase-like activity of $LaNiO_3$-H_2-Air was almost the same as that of the $LaNiO_3$ nanocubes. The recovered catalytic activity of $LaNiO_3$-H_2-Air was attributed to the reoxidized Ni^{3+}, further confirming the importance of Ni^{3+} to the Ni-based nanomaterials' peroxidase mimicking activities.

To study the effect of La atom on the catalytic activity of $LaNiO_3$ nanocubes, the peroxidase mimicking activity of La_2O_3 nanoparticles with the same La^{3+} as $LaNiO_3$ was investigated. As shown in Figure S7, La_2O_3 nanoparticles exhibited nearly negligible activity when compared with $LaNiO_3$ nanocubes, suggesting that the Ni^{3+} instead of La^{3+} played the dominant role in the peroxidase mimicking activity of $LaNiO_3$.

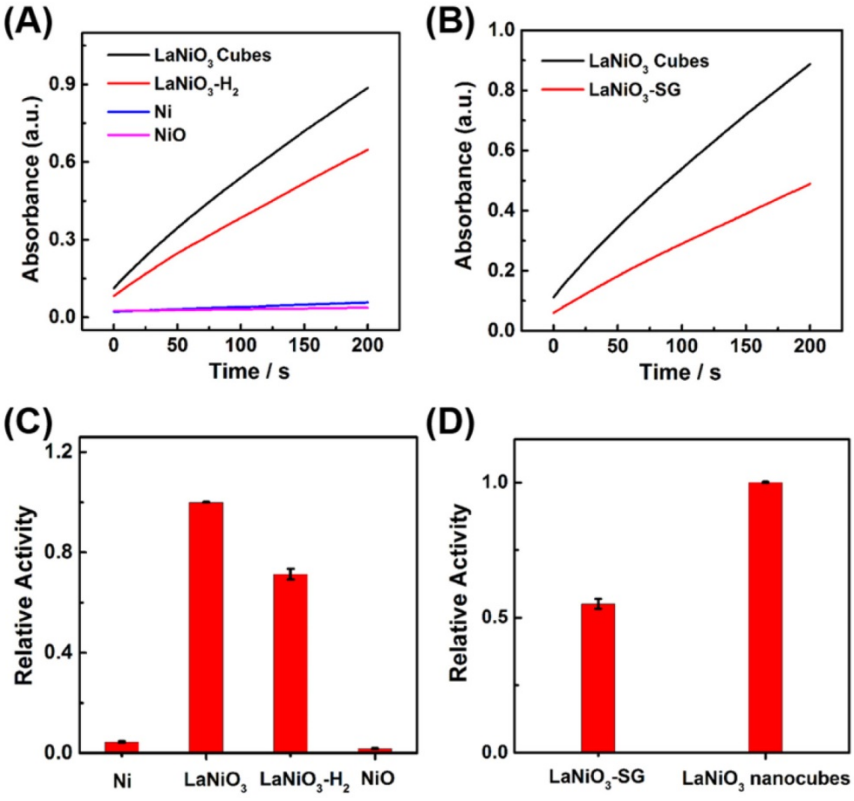

Figure 5. (A, B) Kinetic curves of A_{652} for monitoring the catalytic oxidation of 1 mM TMB with 40 mM H_2O_2 in the presence of 10 μg/mL of (A) $LaNiO_3$, $LaNiO_3$-H_2, Ni, and NiO; and (B) $LaNiO_3$ and $LaNiO_3$-SG. (C, D) Comparison of the peroxidase mimicking activities of (C) Ni, $LaNiO_3$, $LaNiO_3$-H_2, and NiO; and (D) $LaNiO_3$-SG and $LaNiO_3$ nanocubes.

The peroxidase-like activity of $LaNiO_3$-SG was also investigated and compared with that of the porous $LaNiO_3$ nanocubes. The $LaNiO_3$-SG was synthesized via a conventional sol-gel method to form $LaNiO_3$ nanoparticles. Since the $LaNiO_3$-SG and porous $LaNiO_3$ nanocubes had the same 3+ oxidation state but different morphologies, it enabled us to study the morphology effect on the peroxidase-like activities of $LaNiO_3$. Quantitative analysis showed that the porous $LaNiO_3$ nanocubes exhibited about 2-fold higher activity when compared with $LaNiO_3$-SG. The higher activity of porous $LaNiO_3$ nanocubes than $LaNiO_3$-SG may be attributed to the rough surfaces and rich porosity of nanocubes' morphology.

To exclude the effect of surface area on the catalytic activity, we investigated the surface area normalized peroxidase-like activities of Ni-based nanomaterials. As shown in Figure S8A, the surface area normalized results also showed that the oxidation state of nickel atom was very important for the peroxidase-like activity of Ni-based nanomaterials. The Ni^{3+} could be an optimal oxidation state for Ni-based nanomaterials with peroxidase-like activities. As shown in Figure S8B, the $LaNiO_3$ nanocubes showed a higher surface area normalized activity than $LaNiO_3$-SG, suggesting that the effect of morphology on the peroxidase-like activity of nanomaterials. In conclusion, the results obtained from the surface area normalized activity was well agreed with those obtained from mass normalized activity.

Therefore, the porous $LaNiO_3$ nanocubes with the highest peroxidase mimicking activity were obtained by inducing its 3+ oxidation state of nickel atom in $LaNiO_3$ perovskite and optimizing the morphology of nanomaterials.

Detection of H_2O_2, Glucose, and Sarcosine

On the basis of the highest intrinsic peroxidase-like activity of the porous $LaNiO_3$ nanocubes, we developed colorimetric assays for H_2O_2, glucose, and sarcosine detection. As demonstrated above, the peroxidase-like activity of porous $LaNiO_3$ nanocubes was dependent on the H_2O_2 concentrations, which can be used to detect H_2O_2 by monitoring the absorbance of TMB at 652 nm. As seen in Figure S10A and Figure S10B, the intensity of absorption peak at 652 nm increased with the increase of H_2O_2 concentration from 0 μM to 1000 μM. Figure S10C and Figure S10D exhibited good linearity relationships between the absorbance intensity at 652 nm and the H_2O_2 concentrations from 0 μM to 30 μM and 40 μM to 500 μM.

The glucose detection was then carried out by coupling cascade reactions of the glucose oxidation catalyzed by GOx and the TMB oxidation catalyzed by $LaNiO_3$ nanocubes (Figure S11). First, GOx catalyzed the glucose oxidation with O_2 to produce H_2O_2; then, the $LaNiO_3$ nanocubes catalyzed the TMB oxidation with the *in situ* generated H_2O_2. Therefore, glucose could be determined by monitoring the absorbance of TMB at 652 nm. Figure 6A showed that the absorbance intensity exhibited a good response to glucose concentration from 2 μM to 1000 μM. A linear range from 10 μM to 50 μM and a detection limit of 8.16 μM were obtained for glucose detection. Control experiments were performed to evaluate the selectivity of the developed colorimetric assay for glucose by using other sugars such as fructose, lactose, and sucrose. As showed in Figure 6B, the other glucose analogues with a high concentration of 5 mM exhibited a negligible absorbance when compared with that of 1 mM glucose. This result demonstrated that the developed colorimetric assay had a good selectivity for glucose detection because of the high specificity of GOx for catalytic glucose oxidation.

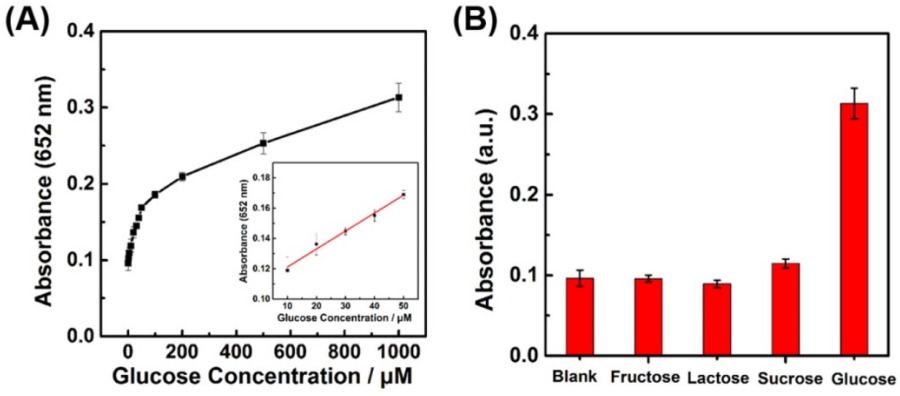

Figure 6. (A) Dependence of A_{652} for monitoring the catalytic oxidation of TMB on the concentration of glucose from 2 μM to 1 mM. The inset shows the linear calibration plot between the concentration of glucose and the absorbance at 652 nm. (B) Selectivity of glucose detection with the porous $LaNiO_3$ nanocubes. Absorbance of TMB at 652 nm in the absence and presence of 5 mM fructose, 5mM lactose, 5 mM sucrose, and 1 mM glucose.

To demonstrate the practical applications of the developed colorimetric assay in real samples, four serum samples from patients were used for glucose detection. As shown in Table S3, the results obtained by our colorimetric assay agreed with the results obtained by a glucose meter, validating the developed colorimetric assay for glucose detection in complicated biomedical samples.

To show the general applications of the porous $LaNiO_3$ nanocubes based colorimetric assays, the sarcosine detection was also performed. By using SOx and $LaNiO_3$ nanocubes catalyzed cascade reaction, the sarcosine concentration could be determined by monitoring the absorbance of TMB at 652 nm (Figure S12). As shown in Figure S13, the absorbance intensity also exhibited a good response to sarcosine concentration from 0.5 μM to 500 μM. A linear range from 0.5 μM to 20 μM and a detection limit of 0.5 μM were obtained for sarcosine detection. The selectivity of the developed colorimetric assay for sarcosine detection was evaluated by using other amino acids such as glutamic acid, histidine, aspartic acid, and lysine. As shown in Figure S14, the other amino acids with a high concentration of 5 mM exhibited a negligible absorbance while sarcosine with a concentration of 1 mM showed a high absorbance, suggesting that the developed colorimetric assay had a good selectivity for sarcosine detection.

Conclusion

In conclusion, we obtained the porous $LaNiO_3$ nanocubes as a peroxidase mimic by optimizing the oxidation state of nickel atom in Ni-based nanomaterials and the morphology of $LaNiO_3$ perovskite oxide. For Ni-based nanomaterials, $LaNiO_3$ perovskite oxide containing 3+ oxidation state showed excellent peroxidase-like activity while the Ni nanoparticles with Ni^0 and NiO with Ni^{2+} exhibited negligible activities, confirming the importance of the oxidation state of nickel atom in Ni-based nanomaterials. More, the porous $LaNiO_3$ nanocubes were more active than the $LaNiO_3$ nanoparticles synthesized by a conventional sol-gel method. The porous $LaNiO_3$ nanocubes followed the typical Michaeli-Menten kinetics and showed the dependence on the temperature, pH, catalyst concentration and H_2O_2 concentration. Based on the peroxidase-like activity of the porous $LaNiO_3$ nanocubes, sensitive and selective colorimetric assays for H_2O_2, glucose, and sarcosine detection have been developed. The porous $LaNiO_3$ nanocubes with high peroxidase-like activity exhibited promising applications in clinical diagnostics.

Supplementary Material

Supplementary figures and tables.
http://www.thno.org/v07p2277s1.pdf

Acknowledgements

This work was supported by National Natural Science Foundation of China (21405081), Natural Science Foundation of Jiangsu Province (BK20130561), 973 Program (2015CB659400), PAPD program, Shuangchuang Program of Jiangsu Province, Open Funds of the State Key Laboratory of Analytical Chemistry for Life Science (SKLACLS1704), Open Funds of the State Key Laboratory of Electroanalytical Chemistry (SKLEAC201501), and Thousand Talents Program for Young Researchers.

Competing Interests

The authors have declared that no competing interest exists.

References

1. Nelson DL, Cox MM. Lehninger Principles of Biochemistry. 5th edition. New York: W. H. Freeman and Company; 2008: 183-229.
2. Breslow R. Artificial Enzymes. Science. 1982; 218: 532-7.
3. Murakami Y, Kikuchi J, Hisaeda Y, Hayashida O. Artificial enzymes. Chem Rev. 1996; 96: 721-58.
4. Breslow R. Artificial enzymes. Wiley-VCH Verlag GmbH & Co KGaA, Weinheim. 2005.
5. Cheng H, Wang X, Wei H. Artificial Enzymes: The Next Wave. In: Wang Z, ed. Encyclopedia of Physical Organic Chemistry, First Edition. John Wiley & Sons, Inc. 2017: 3885-3948.
6. Wei H, Wang EK. Nanomaterials with enzyme-like characteristics (nanozymes): next-generation artificial enzymes. Chem Soc Rev. 2013; 42: 6060-93.
7. Ragg R, Tahir MN, Tremel W. Solids Go Bio: Inorganic Nanoparticles as Enzyme Mimics. Eur J Inorg Chem. 2016;: 1906-15.
8. Gao L, Yan X. Nanozymes: an emerging field bridging nanotechnology and biology. Sci China Life Sci. 2016; 59: 400-2.
9. Melemenidis S, Jefferson A, Ruparelia N, Akhtar AM, Xie J, Allen D, et al. Molecular Magnetic Resonance Imaging of Angiogenesis In Vivo using Polyvalent Cyclic RGD-Iron Oxide Microparticle Conjugates. Theranostics. 2015; 5: 515-29.
10. Wang X, Hu Y, Wei H. Nanozymes in bionanotechnology: from sensing to therapeutics and beyond. Inorg Chem Front. 2016; 3: 41-60.
11. Wang X, Guo W, Hu Y, Wu J, Wei H. Nanozymes: Next Wave of Artificial Enzymes. Springer; 2016.
12. Liu B, Liu J. Surface modification of nanozymes. Nano Research. 2017; 10:1125-48.
13. Manea F, Houillon FB, Pasquato L, Scrimin P. Nanozymes: Gold-nanoparticle-based transphosphorylation catalysts. Angew Chem Int Ed. 2004; 43: 6165-9.
14. Gao L, Zhuang J, Nie L, Zhang J, Zhang Y, Gu N, et al. Intrinsic peroxidase-like activity of ferromagnetic nanoparticles. Nat Nanotechnol. 2007; 2: 577-83.
15. Song Y, Qu K, Zhao C, Ren J, Qu X. Graphene Oxide: Intrinsic Peroxidase Catalytic Activity and Its Application to Glucose Detection. Adv Mater. 2010; 22: 2206-10.
16. Natalio F, Andre R, Hartog AF, Stoll B, Jochum KP, Wever R, et al. Vanadium pentoxide nanoparticles mimic vanadium haloperoxidases and thwart biofilm formation. Nat Nanotechnol. 2012; 7: 530-5.
17. Xia X, Zhang J, Lu N, Kim MJ, Ghale K, Xu Y, et al. Pd-Ir Core-Shell Nanocubes: A Type of Highly Efficient and Versatile Peroxidase Mimic. ACS Nano. 2015; 9: 9994-10004.
18. Cai R, Yang D, Peng S, Chen X, Huang Y, Liu Y, et al. Single Nanoparticle to 3D Supercage: Framing for an Artificial Enzyme System. J Am Chem Soc. 2015; 137: 13957-63.
19. Zhang W, Hu S, Yin J, He W, Lu W, Ma M, et al. Prussian Blue Nanoparticles as Multienzyme Mimetics and Reactive Oxygen Species Scavengers. J Am Chem Soc. 2016; 138: 5860-5.
20. Luo W, Zhu C, Su S, Li D, He Y, Huang Q, et al. Self-Catalyzed, Self-Limiting Growth of Glucose Oxidase-Mimicking Gold Nanoparticles. ACS Nano. 2010; 4: 7451-8.

21. Zheng X, Liu Q, Jing C, Li Y, Li D, Luo W, et al. Catalytic Gold Nanoparticles for Nanoplasmonic Detection of DNA Hybridization. Angew Chem Int Ed. 2011; 50: 11994-8.
22. Vernekar AA, Sinha D, Srivastava S, Paramasivam PU, D'Silva P, Mugesh G. An antioxidant nanozyme that uncovers the cytoprotective potential of vanadia nanowires. Nat Commun. 2014; 5: 5301.
23. Shen X, Liu W, Gao X, Lu Z, Wu X, Gao X. Mechanisms of Oxidase and Superoxide Dismutation-like Activities of Gold, Silver, Platinum, and Palladium, and Their Alloys: A General Way to the Activation of Molecular Oxygen. J Am Chem Soc. 2015; 137: 15882-91.
24. Tonga GY, Jeong Y, Duncan B, Mizuhara T, Mout R, Das R, et al. Supramolecular regulation of bioorthogonal catalysis in cells using nanoparticle-embedded transition metal catalysts. Nat Chem. 2015; 7: 597-603.
25. Zhao Y, Huang Y, Zhu H, Zhu Q, Xia Y. Three-in-One: Sensing, Self-Assembly, and Cascade Catalysis of Cyclodextrin Modified Gold Nanoparticles. J Am Chem Soc. 2016; 138: 16645-54.
26. Lin Y, Li Z, Chen Z, Ren J, Qu X. Mesoporous silica-encapsulated gold nanoparticles as artificial enzymes for self-activated cascade catalysis. Biomaterials. 2013; 34: 2600-10.
27. Lin Y, Ren J, Qu X. Nano-Gold as Artificial Enzymes: Hidden Talents. Adv Mater. 2014; 26: 4200-17.
28. Wei H, Wang E. Fe_3O_4 magnetic nanoparticles as peroxidase mimetics and their applications in H_2O_2 and glucose detection. Anal Chem. 2008; 80: 2250-4.
29. Liu B, Han X, Liu J. Iron oxide nanozyme catalyzed synthesis of fluorescent polydopamine for light-up Zn^{2+} detection. Nanoscale. 2016; 8: 13620-6.
30. Fan K, Cao C, Pan Y, Lu D, Yang D, Feng J, et al. Magnetoferritin nanoparticles for targeting and visualizing tumour tissues. Nat Nanotechnol. 2012; 7: 459-64.
31. Tao Y, Ju E, Ren J, Qu X. Bifunctionalized Mesoporous Silica-Supported Gold Nanoparticles: Intrinsic Oxidase and Peroxidase Catalytic Activities for Antibacterial Applications. Adv Mater. 2015; 27: 1097-104.
32. Xue T, Peng B, Xue M, Zhong X, Chiu C-Y, Yang S, et al. Integration of molecular and enzymatic catalysts on graphene for biomimetic generation of antithrombotic species. Nat Commun. 2014; 5: 3200.
33. Gao L, Giglio KM, Nelson JL, Sondermann H, Travis AJ. Ferromagnetic nanoparticles with peroxidase-like activity enhance the cleavage of biological macromolecules for biofilm elimination. Nanoscale. 2014; 6: 2588-93.
34. Kim CK, Kim T, Choi I-Y, Soh M, Kim D, Kim Y-J, et al. Ceria Nanoparticles that can Protect against Ischemic Stroke. Angew Chem Int Ed. 2012; 51: 11039-43.
35. Kwon HJ, Cha M-Y, Kim D, Kim DK, Soh M, Shin K, et al. Mitochondria-Targeting Ceria Nanoparticles as Antioxidants for Alzheimer's Disease. ACS Nano. 2016; 10: 2860-70.
36. Zhang Y, Wang Z, Li X, Wang L, Yin M, Wang L, et al. Dietary Iron Oxide Nanoparticles Delay Aging and Ameliorate Neurodegeneration in Drosophila. Adv Mater. 2016; 28: 1387-93.
37. Chen ZW, Yin JJ, Zhou YT, Zhang Y, Song L, Song MJ, et al. Dual Enzyme-like Activities of Iron Oxide Nanoparticles and Their Implication for Diminishing Cytotoxicity. ACS Nano. 2012; 6: 4001-12.
38. Xiong F, Wang H, Feng Y, Li Y, Hua X, Pang X, et al. Cardioprotective activity of iron oxide nanoparticles. Sci Rep. 2015; 5.
39. Dong J, Song L, Yin J-J, He W, Wu Y, Gu N, et al. Co_3O_4 Nanoparticles with Multi-Enzyme Activities and Their Application in Immunohistochemical Assay. ACS Appl Mat Interfaces. 2014; 6: 1959-70.
40. Wu G, He S, Peng H, Deng H, Liu A, Lin X, et al. Citrate-Capped Platinum Nanoparticle as a Smart Probe for Ultrasensitive Mercury Sensing. Anal Chem. 2014; 86: 10955-60.
41. Shi W, Wang Q, Long Y, Cheng Z, Chen S, Zheng H, et al. Carbon nanodots as peroxidase mimetics and their applications to glucose detection. Chem Commun. 2011; 47: 6695-7.
42. Duan D, Fan K, Zhang D, Tan S, Liang M, Liu Y, et al. Nanozyme-strip for rapid local diagnosis of Ebola. Biosens Bioelectron. 2015; 74: 134-41.
43. Liu Q, Yang Y, Li H, Zhu R, Shao Q, Yang S, et al. NiO nanoparticles modified with 5,10,15,20-tetrakis(4-carboxyl pheyl)-porphyrin: Promising peroxidase mimetics for H_2O_2 and glucose detection. Biosens Bioelectron. 2015; 64: 147-53.
44. He W, Wu X, Liu J, Hu X, Zhang K, Hou S, et al. Design of AgM Bimetallic Alloy Nanostructures (M = Au, Pd, Pt) with Tunable Morphology and Peroxidase-Like Activity. Chem Mater. 2010; 22: 2988-94.
45. Liu S, Lu F, Xing R, Zhu J. Structural Effects of Fe_3O_4 Nanocrystals on Peroxidase-Like Activity. Chem Euro J. 2011; 17: 620-5.
46. Ge C, Fang G, Shen X, Chong Y, Wamer WG, Gao X, et al. Facet Energy versus Enzyme-like Activities: The Unexpected Protection of Palladium Nanocrystals against Oxidative Damage. ACS Nano. 2016; 10: 10436-45.
47. Wang S, Chen W, Liu A, Hong L, Deng H, Lin X. Comparison of the Peroxidase-Like Activity of Unmodified, Amino-Modified, and Citrate-Capped Gold Nanoparticles. ChemPhysChem. 2012; 13: 1199-204.
48. Fan K, Wang H, Xi J, Liu Q, Meng X, Duan D, et al. Optimization of Fe_3O_4 nanozyme activity via single amino acid modification mimicking an enzyme active site. Chem Commun. 2016; 53: 424-7.
49. Cheng H, Lin S, Muhammad F, Lin Y-W, Wei H. Rationally Modulate the Oxidase-like Activity of Nanoceria for Self Regulated Bioassays. ACS Sensors. 2016; 1: 1336-43.
50. Heckert EG, Karakoti AS, Seal S, Self WT. The role of cerium redox state in the SOD mimetic activity of nanoceria. Biomaterials. 2008; 29: 2705-9.
51. Pirmohamed T, Dowding JM, Singh S, Wasserman B, Heckert E, Karakoti AS, et al. Nanoceria exhibit redox state-dependent catalase mimetic activity. Chem Commun. 2010; 46: 2736-8.
52. Liu B, Huang Z, Liu J. Boosting the oxidase mimicking activity of nanoceria by fluoride capping: rivaling protein enzymes and ultrasensitive F^- detection. Nanoscale. 2016; 8: 13562-7.
53. Zhang X-Q, Gong S-W, Zhang Y, Yang T, Wang C-Y, Gu N. Prussian blue modified iron oxide magnetic nanoparticles and their high peroxidase-like activity. J Mater Chem. 2010; 20: 5110-6.
54. Xiong R, Soenen SJ, Braeckmans K, Skirtach AG. Towards Theranostic Multicompartment Microcapsules: in-situ Diagnostics and Laser-induced Treatment. Theranostics. 2013; 3: 141-51.
55. Cheng H, Wang X, Wei H. Ratiometric Electrochemical Sensor for Effective and Reliable Detection of Ascorbic Acid in Living Brains. Anal Chem. 2015; 87: 8889-95.
56. Sun X, Guo S, Chung C-S, Zhu W, Sun S. A Sensitive H_2O_2 Assay Based on Dumbbell-like PtPd-Fe_3O_4 Nanoparticles. Adv Mater. 2013; 25: 132-6.
57. Qian C, Chen Y, Zhu S, Yu J, Zhang L, Feng P, et al. ATP-Responsive and Near-Infrared-Emissive Nanocarriers for Anticancer Drug Delivery and Real-Time Imaging. Theranostics. 2016; 6: 1053-64.
58. Zhang P, Chen Y, Zeng Y, Shen C, Li R, Guo Z, et al. Virus-mimetic nanovesicles as a versatile antigen-delivery system. Proc Natl Acad Sci USA. 2015; 112: E6129-E38.
59. Cheng H, Zhang L, He J, Guo W, Zhou Z, Zhang X, et al. Integrated Nanozymes with Nanoscale Proximity for in Vivo Neurochemical Monitoring in Living Brains. Anal Chem. 2016; 88: 5489-97.
60. Liu B, Sun Z, Huang P-JJ, Liu J. Hydrogen Peroxide Displacing DNA from Nanoceria: Mechanism and Detection of Glucose in Serum. J Am Chem Soc. 2015; 137: 1290-5.
61. Gu Z, Dang TT, Ma M, Tang BC, Cheng H, Jiang S, et al. Glucose-Responsive Microgels Integrated with Enzyme Nanocapsules for Closed-Loop Insulin Delivery. ACS Nano. 2013; 7: 6758-66.
62. Yu J, Zhang Y, Ye Y, DiSanto R, Sun W, Ranson D, et al. Microneedle-array patches loaded with hypoxia-sensitive vesicles provide fast glucose-responsive insulin delivery. Proc Natl Acad Sci USA. 2015; 112: 8260-5.
63. He H, Xu X, Wu H, Jin Y. Enzymatic Plasmonic Engineering of Ag/Au Bimetallic Nanoshells and Their Use for Sensitive Optical Glucose Sensing. Adv Mater. 2012; 24: 1736-40.
64. Chen L, Li H, He H, Wu H, Jin Y. Smart Plasmonic Glucose Nanosensors as Generic Theranostic Agents for Targeting-Free Cancer Cell Screening and Killing. Anal Chem. 2015; 87: 6868-74.
65. Fan W, Lu N, Huang P, Liu Y, Yang Z, Wang S, et al. Glucose-Responsive Sequential Generation of Hydrogen Peroxide and Nitric Oxide for Synergistic Cancer Starving-Like/Gas Therapy. Angew Chem Int Ed. 2017; 56: 1229-33.
66. Sreekumar A, Poisson LM, Rajendiran TM, Khan AP, Cao Q, Yu J, et al. Metabolomic profiles delineate potential role for sarcosine in prostate cancer progression. Nature. 2009; 457: 910-4.
67. Zhang J, Zhao Y, Zhao X, Liu Z, Chen W. Porous Perovskite $LaNiO_3$ Nanocubes as Cathode Catalysts for Li-O_2 Batteries with Low Charge Potential. Sci Rep. 2014; 4: 6005.
68. Liu H, More R, Grundmann H, Cui C, Erni R, Patzke GR. Promoting Photochemical Water Oxidation with Metallic Band Structures. J Am Chem Soc. 2016; 138: 1527-35.
69. Mahaleh YBM, Sadrnezhaad SK, Hosseini D. NiO Nanoparticles Synthesis by Chemical Precipitation and Effect of Applied Surfactant on Distribution of Particle Size. J Nanomater. 2008; 2008: 470595.